RSC Advances

PAPER

View Article Online
View Journal | View Issue

Cite this: RSC Adv., 2015, 5, 78128

In,V-codoped TiO_2 nanocomposite prepared *via* a photochemical reduction technique as a novel high efficiency visible-light-driven nanophotocatalyst

V. Jabbari,*[a] M. Hamadanian,*[bc] A. Reisi-Vanani,[c] P. Razi,[c] S. Hoseinifard[c] and D. Villagrán[a]

In the current study, a series of novel, high efficiency photocatalysts of In,V-codoped TiO_2 were developed. The TiO_2 nanoparticles were synthesized by sol–gel and hydrothermal methods and different molar percentages (0.1–1%) of vanadium (V) and Indium (In) nanoclusters were deposited over the TiO_2 nanoparticles *via* photochemical reduction. XRD, SEM, EDX, TEM, XPS and UV-vis DRS analyses were carried out to characterize the prepared In,V-codoped TiO_2 nanocatalysts, and methyl orange (MO) was used as the probe environmental pollutant to test the photocatalytic performance of the prepared catalysts under UV and visible light irradiation. Our study demonstrated that In and V nanoclusters were successfully deposited over TiO_2 particles *via* a photochemical deposition technique and the metal doping slightly suppressed TiO_2 crystal growth. The optical analysis showed a red shift in the light absorption spectrum and decrease in the band gap of In,V-codoped TiO_2 catalysts compared to that of parent TiO_2. XPS study revealed that the doped elements In and V are in oxidation state of 3 (In^{III}), 4 (V^{IV}) and 5 (V^{V}). The photo-oxidative decomposition of MO showed that doping of In and V can considerably improve the photocatalytic activity of TiO_2. Thus, for the first time, we demonstrated that TiO_2 codoped with binary metals of In and V can serve as a high efficiency visible-light-active photocatalyst.

Received 6th July 2015
Accepted 24th August 2015

DOI: 10.1039/c5ra13179k

www.rsc.org/advances

1. Introduction

In recent years, many attempts have been devoted for developing heterogeneous photocatalysts with high activity for environmental applications, including water disinfection, water purification, air purification and hazardous waste remediation.[1,2] Among the various metal oxide semiconductor photocatalysts, TiO_2 has shown to be the most suitable for environmental purposes due to its strong oxidizing power, chemical inertness, long-term stability, and cost effectiveness.[3,4] The primary event occurring on the TiO_2 surface after irradiation is the generation of electrons (e_{CB}^-) and holes (h_{VB}^+). In these reactions, the organic pollutants are oxidized (decomposed) by the photogenerated h_{VB}^+ or by the reactive oxygen species ($OH^\bullet$ and O_2^- radicals) formed on the illuminated TiO_2 surface. However, the practical application of TiO_2 is limited by two main factors. First, due to the wide band gap of TiO_2 (3.2 eV for anatase, 3.0 eV for rutile phase),[5] it can only absorb the UV portion of solar light (λ < 387 nm), which is up to 5% of solar light.[6] Therefore, to extend its practical application, many efforts have been made to design second-generation TiO_2-based photocatalysts, which would be able to induce photocatalysis under visible light irradiation. Second, the low rate of photocatalytic decomposition using TiO_2 photocatalyst is attributed to the charge recombination of photogenerated electron–hole pairs (charge carriers).

To overcome these problems, several approaches have been proposed: metal doping,[7,8] metal ion doping,[9–11] nonmetal doping,[12–14] dye-sensitizing of TiO_2 (*e.g.* thionine),[15,16] fabricating composites of TiO_2 with other semiconductors with a narrow band gap energy (*e.g.* CdS particles),[17] and doping TiO_2 with an up-conversion luminescence agent.[18] Among these, metal doping has been proved to be a very promising approach as it greatly extends the light absorption of TiO_2 and significantly improves the trapping efficiency of change carriers.[19–22]

Raftery *et al.*, reported that doping TiO_2 nanoparticles with vanadium cations could extend the photoresponse of TiO_2 to the visible light region (396–450 nm) and also temporarily trap the photogenerated electrons (e^-) and holes (h^+), thus suppressing the recombination of the charge carriers.[23] Wu and Chen found that V-doped TiO_2 exhibits photoactivity in the visible light region and shows a "red shift" in the UV-vis spectra.[24] Choi *et al.*, reported that doping V^{4+} into TiO_2 at V/Ti ratio of 0.1–0.5 wt% can significantly increase the TiO_2 photoreactivity due to the improved interfacial charge transfer.[25]

[a]Department of Chemistry, The University of Texas at El Paso, El Paso, Texas 79968, USA. E-mail: vjabbari86@gmail.com; vahid_jabbari.azeri@yahoo.com
[b]Institute of Nanosciences and Nanotechnology, University of Kashan, Kashan, Iran. E-mail: hamadani@kashanu.ac.ir; Fax: +98 31 55912397; Tel: +98 31 55912382
[c]Department of Physical Chemistry, Faculty of Chemistry, University of Kashan, Kashan, Iran

Wang *et al.*, observed that by introducing In ions into the TiO_2 structure, not only new energy states emerge between the TiO_2 band gap, which results in considerable red shift in absorption, but also the ions facilitate the charge separation.[26] The same results were reported by another group.[27] They analyzed the photocatalytic activity of In-doped TiO_2 under visible light illumination. It was demonstrated that the In doping improved visible light response of the TiO_2 catalyst and enhanced the charge carrier separation, which when combined leads to significant improvement in the photocatalytic performance of TiO_2 under visible light illumination.

Modification of TiO_2 by binary doping of metal ions is a novel process for enhancing the optical efficiency of TiO_2. The synergic effect of codoping can further improve the photocatalytic activity of TiO_2. Recently, a number of literatures have reported different types of photocatalysts using binary metal-doped TiO_2. Estrellan *et al.* synthesized Fe,Nb-codoped TiO_2 *via* the sol–gel method.[28] Fe–Nb–TiO_2 exhibited the anatase crystalline phase with high values of crystallinity along with a red shift in light absorption. It was reported that TiO_2 co-doping with cations of Rh^{3+}/Sb^{5+} can result in a greatly improved photocatalytic activity.[29] Zhang *et al.*, prepared V,Sc-codoped TiO_2 by the sol–gel method and found that binary doping of these metals led to a considerable decline in the charge recombination and also induced a large red shift in the TiO_2 absorption spectrum.[30]

The photochemical reduction method has recently attracted considerable attention due to its versatile advantages: (i) controlled reduction of metal ions can be carried out without using an excess of a reducing agent, (ii) the reduction reaction is uniformly performed in the solution, and (iii) light radiation is absorbed regardless of the presence of light absorbing solutes and products.[31]

The aim of the current study, which to the best of our knowledge is for the first time, is to study the synergistic effect of co-doping In and V ions on the photocatalytic activity of TiO_2 nanoparticles. The physicochemical characteristic of the prepared catalysts were investigated by XRD, SEM, EDX, TEM, XPS and UV-vis DRS. Methyl orange (MO) was used as the probe organic pollutant to monitor the photocatalytic performance of the In,V-codoped TiO_2 catalysts. Finally, it is found that the In,V-codoped TiO_2 shows a size in the nanometer range with strong light absorbance and high quantum efficiency of charge carriers and the 0.2% In–0.2% V/TiO_2 catalyst exhibited superior photocatalytic activity compared to parent TiO_2, under UV and visible light irradiation.

2. Experimental

2.1. Chemicals

Titanium(IV) tetraisopropoxide (TTIP, $Ti[OCH(CH_3)_4]_4$ (Merck, >98%)), glacial acetic acid (Merck, >99.8%), vanadium chloride (VCl_3, Merck), and indium chloride ($InCl_3$, Merck) were used as received without further purification. Deionized water was prepared by an ultra pure water system (Smart-2-Pure, TKA Co, Germany). Methyl orange (MO, M.W. = 695.58 g mol^{-1}) was provided by Alvan Co., Iran.

2.2. Synthesis of pure TiO_2 nanoparticles by hydrothermal and sol–gel methods

Pure TiO_2 nanoparticles were prepared according to previous studies by sol–gel[32] and hydrothermal[33] methods. TiO_2 nanoparticles prepared by hydrothermal and sol–gel processes were calcined at 450 °C for 3 h and 500 °C for 2 h, respectively.

2.3. Preparation of In–TiO_2 and In,V-codoped TiO_2 nanoparticles *via* photochemical reduction

The photochemical route is a promising way to form noble metal–semiconductor nanocomposites *in situ* by reducing noble metal ions adsorbed on the surface of a semiconductor. It is well known that a semiconductor can be excited to generate electrons (e^-) and holes (h^+) in the conduction band (CB) and valence band (VB), respectively, if the energy of the photons of the incident light is larger than that of the band gap of the semiconductor.[34] The metal ion dopants influence the photoefficiency of TiO_2 by acting as electron or hole trap centres within the band gap of TiO_2 and alter the e^-/h^+ pair recombination rate[32] through the following process. The photoreduction of the metal ions (eqn (1)) is accompanied by the elimination of photo-generated holes by water oxidation (eqn (2)):

$$M^{n+} + ne^- \rightarrow M^o \quad (1)$$

$$2H_2O + 4h^+ \rightarrow O_2 + 4H^+ \quad (2)$$

In-doped TiO_2 with varying metal content was prepared as follows:

To prepare In-doped TiO_2, first different molar percent of $InCl_3$ (0.1, 0.2%, 0.4%, 0.6%, 1.0% of In to Ti molar ratio) as the indium source was added to 100 ml of aqueous solution containing a certain amount of pure TiO_2 particles synthesized by sol–gel and hydrothermal processes. Then, the resulting solution was purged with a high-purity N_2 atmosphere while stirring. Furthermore, the resulting solution was transferred to a quartz reactor with its head covered and was placed under UV irradiation for 12 h, under vigorous stirring. After this stage, the precursor was filtered by centrifugation and washed with deionized water several times. The resulting powders were dried at 100 °C for 12 h.

To prepare In,V-codoped TiO_2, the same method for synthesis of In-doped TiO_2 was adopted using both $InCl_3$ (0.1%, 0.2%, 0.4%, 0.6%, 1.0% of In to Ti molar ratio) as the indium source and VCl_3 (0.1%, 0.2%, 0.4%, 0.6%, 1.0% of V to Ti molar ratio) as the vanadium source.

2.4. Characterization of the prepared catalysts

Crystalline phases of the prepared samples were analysed by X-ray powder diffraction (XRD, Bruker D8 Discover X-ray Diffractometer). The morphology was investigated by a transmission electron microscope (TEM, JEOL JEM3200 FS) and a scanning electron microscope (SEM, Hitachi S-4800) equipped with an energy dispersive X-ray detector (EDX). UV-vis DRS spectra of the samples were obtained by a Shimadzu 1800 spectrometer.

UV-vis absorption spectra of MO degradation were obtained by UV-vis spectrophotometer (Perkin Elmer Lambda2S, Germany). XPS test was monitored by an Omicron XPS/UPS system with an Argus detector, which uses an Omicron's DAR 400 dual Mg/Al X-ray source.

2.5. Photocatalytic performance analysis

The photocatalytic activity of the prepared catalysts was analyzed by MO degradation under UV and visible light irradiation. Each time, 0.1 g photocatalyst was dispersed into 100 ml MO aqueous solution with a concentration of 10 mg l^{-1} held in a quartz reactor (with a dimension of 12 cm × 5 cm, height and diameter, respectively). Two 400 W Osram lamps provided the visible and UV sources, located 40 cm and 25 cm away from the reactor, respectively. The reaction system was stirred in the dark for 30 min to achieve absorption equilibrium before irradiation.

3. Results and discussion

3.1. X-ray diffraction patterns

Fig. 1 shows the XRD patterns of parent TiO_2 and In,V-codoped TiO_2 catalysts. (101), (004), (200), (105), (211), (204) and (116) diffraction peaks were proof of the anatase phase for pure TiO_2.[35] A main peak for anatase around $2\theta = 25.2°$ (101) has a tetragonal form.[35] Moreover, no rutile phase diffraction peaks were detected in the samples. Furthermore, the XRD pattern did not show any In or V phase (as in metallic or metal oxide states) and it was concluded that In and V ions were uniformly loaded onto the TiO_2 surface. There is also a relatively small shift in In,V-codoped TiO_2 compared to parent TiO_2, which shows slight distortion in the TiO_2 structure.

Debye–Scherrer formula was used for measuring the average crystallite size of the prepared catalysts as follows:

$$D = k\lambda/\beta \cos\theta \quad (3)$$

where k is the constant taken as 0.9 here, λ is the wavelength of the X-ray radiation (λ = 0.1541 nm), β is the corrected band broadening [(FWHM) full-width at half-maximum] after subtraction of equipment broadening and θ is the Bragg angle.[35] By using this equation on the anatase phase ($2\theta = 25.2°$, 48.2° and 55.2°), the average particle size was calculated for pure TiO_2 synthesized *via* the hydrothermal method to be about 18.75 nm. The particle size of In,V-codoped TiO_2 with 0.2 mol% metal content was estimated to be 14.3 nm. We evidently found that doping TiO_2 by In and V ions results in a decrease of the TiO_2 catalyst particle size.

Indeed, the formation of Ti–O–In or Ti–O–V inhibits the transition of the TiO_2 phase and blocks Ti–O species at the interface with TiO_2 domains, thus preventing the agglomeration of TiO_2 particles. Hence, the doping of TiO_2 by In and V minimizes the charge carrier recombination during the photocatalytic decomposition of MO, and as a result, it is expected that In,V-codoped TiO_2 shows a higher photocatalytic activity compared to pure TiO_2.

3.2. SEM-EDX analysis

Fig. 2 shows SEM micrographs of pure TiO_2 and 0.2% In–0.2% V/TiO_2 catalysts. The SEM micrographs show that the particles consist of uniform, globular and slightly agglomerated particles, and the doped metal ions had no obvious influence on the morphology of the samples. Further observation indicates that the morphology of samples is very rough, which may be beneficial to enhance the adsorption of dye due to its great surface roughness and high surface area.[36] Both narrow size distribution of nanoparticles and optimal dispersion are favourable for photoactivity.

The EDX measurement was carried out to verify the formation of In and V nanoclusters onto the TiO_2 surface after photochemical reduction. As it is obvious from Fig. 3, new peaks appear in the TiO_2 spectra after metal deposition, which confirms the presence of In and V in the prepared In,V/TiO_2 sample.

3.3. TEM analysis

TEM images of pure TiO_2 and 0.2% In–0.2%V/TiO_2 catalysts are shown in Fig. 4. Based on the images, the particle size of the

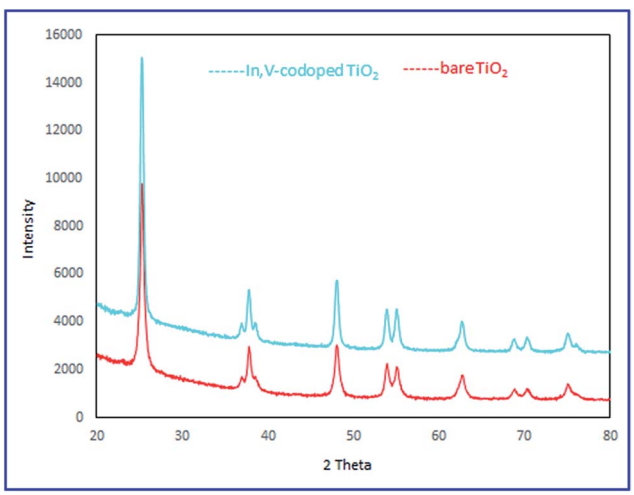

Fig. 1 XRD patterns of parent TiO_2 and In,V-codoped TiO_2 catalysts.

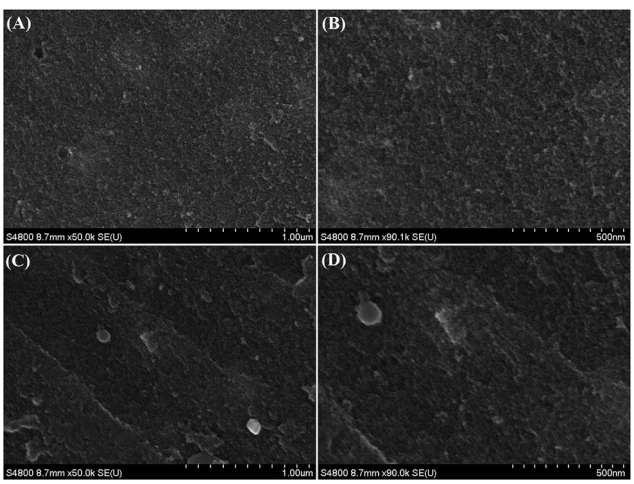

Fig. 2 SEM micrographs of pure TiO_2 (A and B) and In,V-codoped TiO_2 (C and D).

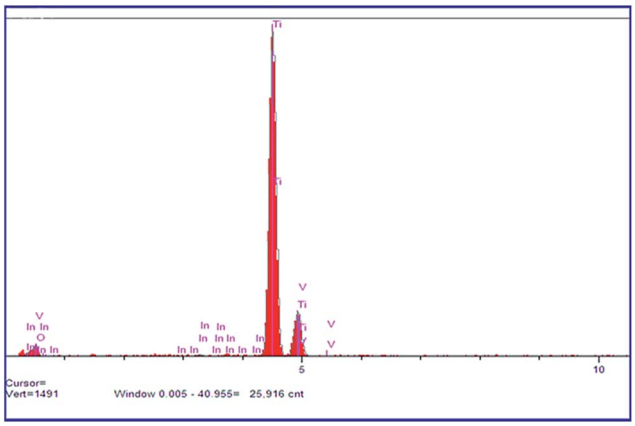

Fig. 3 EDX result of In,V-codoped TiO_2.

0.2% In–0.2% V/TiO_2 sample was estimated to be around 11–13 nm, which is in a good agreement with the particle size estimated from the Debye–Scherrer formula (12–15 nm). Moreover, the HRTEM image shows that the peak located at 2theta = 25° matches well with the (101) plane of anatase TiO_2 (JCPDS card no. 01-065-9124), indicating the formation of anatase TiO_2.[37]

3.4. XPS study of the In,V-codoped TiO_2 catalyst

XPS is carried out to determine the oxidation states of In and V in the In,V-codoped TiO_2 catalyst. Fig. 5 shows the XPS spectrum for In 3d and V 2p of In,V-codoped TiO_2. As shown in Fig. 5, XPS spectrum in Ti 2p region of In,V-codoped TiO_2 shows peaks at around 456 eV (Ti $2p_{3/2}$) and 462 eV (Ti $2p_{1/2}$), which corresponds to Ti^{4+} ions in the TiO_2 lattice.[38] The O 1s peak of the prepared In,V-codoped TiO_2 can be seen at a binding energy of around 527 eV, which is attributed to crystal lattice oxygen (O^{2-}) of In,V-codoped TiO_2 (Ti–O–Ti; Ti–O–In; Ti–O–V).[38]

Our findings show that In in In,V-codoped TiO_2 exists in oxidation state of 3, In(III), showing peaks around 444.8 eV (In $3d_{5/2}$) and 450.6 eV (In $3d_{3/2}$), which is in agreement with previous reports.[39] Regarding the presence of V in the In,V-codoped TiO_2 catalyst, we witnessed a peak for V $2p_{3/2}$, which

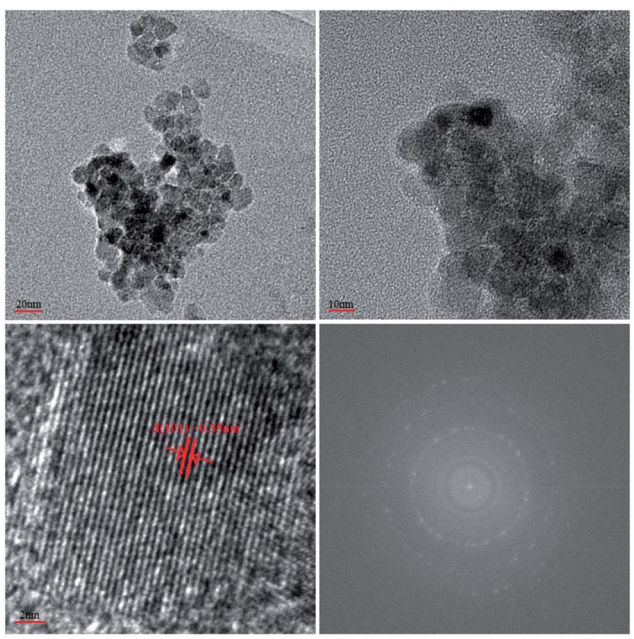

Fig. 4 HRTEM images of In,V-codoped TiO_2.

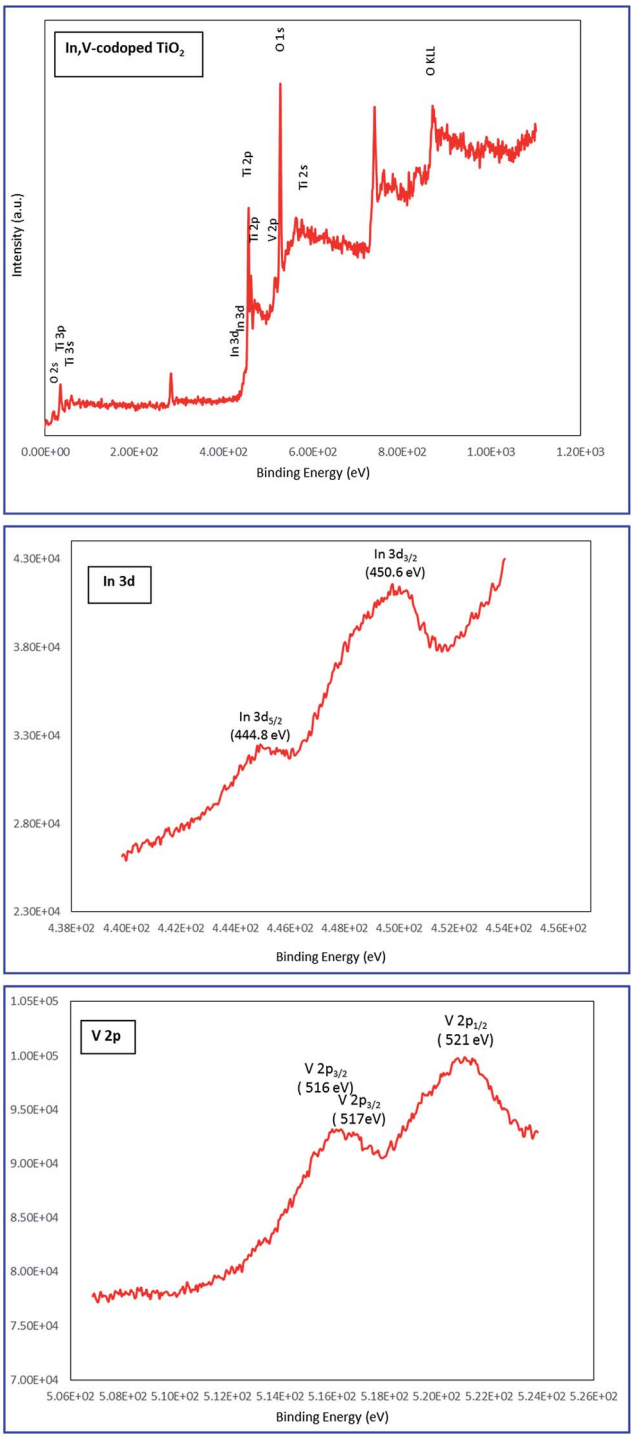

Fig. 5 XPS spectra of In,V-codoped TiO_2.

consists of two peaks, one at around 516 eV, related to V^{4+} and around 517 eV, related to V^{5+}.[38]

3.5. UV-vis DRS analysis of In,V-codoped TiO_2 catalysts

It is well-known that the photocatalytic performance of a metal oxide semiconductor is closely related to its band gap structure. The UV-vis absorbance spectra of the pure and metal doped TiO_2 samples are shown in Fig. 6. By considering the absorbance spectra of pure TiO_2, the onset of the absorption appears at 380 nm, which matches well with the intrinsic band gap of anatase TiO_2 (3.2 eV). Moreover, it is obvious that there is a considerable shift in the absorption toward a higher wavelength for the In,V-codoped TiO_2 catalyst compared to pure TiO_2. The reason for that might be attributed to the appearance of the new electronic energy state in the middle of the TiO_2 band gap, which results in gap reduction between the conduction band (CB) and valence band (VB) of TiO_2, allowing TiO_2 to absorb visible light.[36]

The band gap values of the pure TiO_2 and In,V-codoped TiO_2 catalysts were calculated[40] using the following equation:

$$E_g = h \times c/\lambda \quad (4)$$

where E_g = band gap energy, h = Planck's constant in eV (4.135×10^{-15} eV), c = velocity of light (3×10^8 m s^{-1}), λ = wavelength of the band gap for corresponding catalysts. We found that the band gap values were lower for the doped catalysts (below 3 eV) compared to the pure TiO_2 catalyst (up to 3 eV).

Furthermore, the V 3d energy state and In 4d energy state play important roles in interfacial charge transfer and elimination of charge recombination. Thus, transition metal ions (V and In) would act as efficient electrons scavenger to trap the electrons of CB state of TiO_2.[35] Accordingly, it can be presumed that the In,V–TiO_2 photocatalyst may demonstrate higher photocatalytic activity under visible light irradiation, compared to the pure TiO_2.

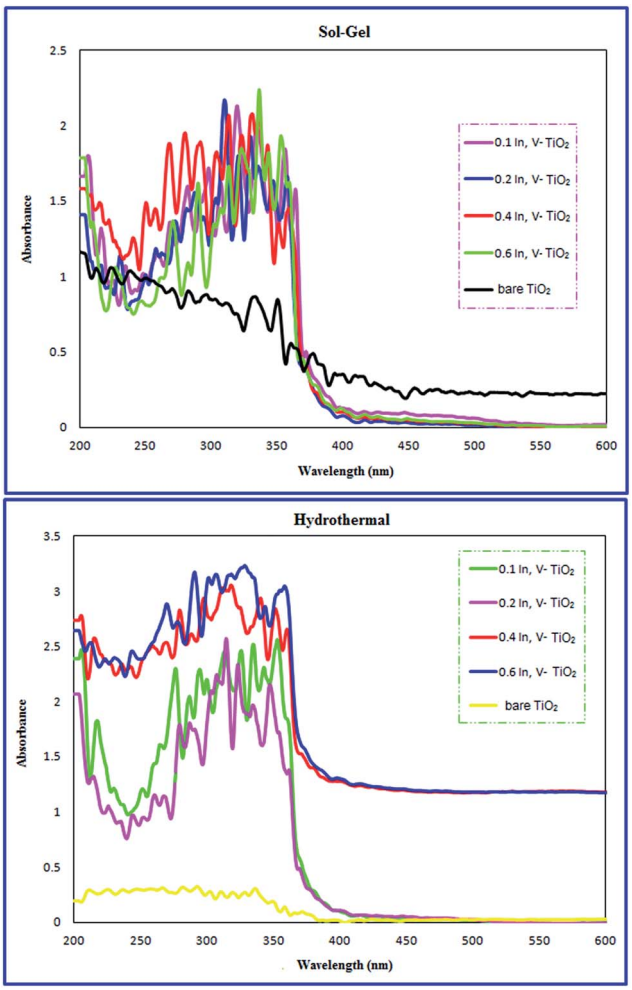

Fig. 6 UV-vis DRS absorption spectra of as-prepared TiO_2 and In,V-codoped TiO_2 nanoparticles with different metal content.

3.6. Photocatalytic performance of In,V-codoped TiO_2 catalysts

Methyl orange (MO) was used as a probe environmental pollutant to study the photocatalytic activity of the pure TiO_2 and metal-doped TiO_2 catalysts. Tables 1 and 2 show the degradation results over In-doped TiO_2 with various metal content synthesized *via* hydrothermal-assisted photochemical reduction and sol–gel assisted photochemical reduction, respectively, and Fig. 7 and 8 demonstrate the photocatalytic

Table 1 The photocatalytic results of MO degradation using In-doped TiO_2 nanoparticles with various In(III) content, prepared *via* hydrothermal assisted photochemical deposition

UV light illumination				
Time (min)	15	30	60	45
Elem. (%)				
0	37.32	59.77	81.07	90.80
0.05	43.91	59.78	75.71	82.56
0.1	35.42	48.58	67.82	82.68
0.2	52.41	71.72	86.51	95.09
0.5	46.28	81.99	88.66	98.47
0.8	45.21	78.47	88.12	96.17
1	38.16	60.69	81.53	92.18
2	44.67	64.37	81.23	92.87

Visible light illumination					
Time (min)	30	60	90	120	150
Elem. (%)					
0	23.85	34.81	48.15	62.98	69.38
0.05	26.15	44.56	60.15	74.21	79.81
0.1	28.66	48.89	70.81	93.55	98.89
0.2	28.89	46.07	61.63	77.63	82.78
0.5	9.18	22.96	36.15	47.48	52.72
0.8	8.02	19.51	29.63	41.52	48.21
1	21.48	37.18	51.48	66.07	72.13
2	26.89	43.11	58.59	73.19	78.32

performance of In,V-codoped TiO_2 with various metals content synthesized *via* sol–gel assisted photochemical reduction and hydrothermal-assisted photochemical reduction, respectively. Before the exposure to UV or visible light on the catalysts, the MO solution containing the catalysts was stirred in dark for half an hour. Our detection results exhibited that the MO concentration showed negligible decrease due to slight absorption on the photocatalysts surface, which showed that there was almost no MO decomposition in the absence of light irradiation.

As it is apparent from Table 1, all In-doped TiO_2 nanoparticles are visible light active. The optimal dosage of indium ion to obtain the highest photocatalytic activity for MO decomposition was found to be 0.1% (hydrothermal-assisted photodeposition) and 0.2% (sol–gel assisted photodeposition) under visible light and 0.5% (hydrothermal-assisted photodeposition) and 2% (sol–gel assisted photodeposition) under UV light illumination.

Our findings for the In,V-codoped TiO_2 catalyst prepared with the sol–gel assisted photodeposition technique (Fig. 7) illustrate no improvement in photocatalytic performance in comparison to pure TiO_2. However, in the case of the In,V-codoped TiO_2 catalyst prepared with the hydrothermal-assisted photodeposition technique (Fig. 8), we found that the TiO_2 catalyst with 0.2% metal content achieved higher rates of MO decomposition compared to the pure TiO_2 catalyst. Indeed, in the In,V-codoped TiO_2 catalyst, the metal could act as an electron trapper and thus reduce the charge recombination rate, which favours the photocatalytic activity enhancement. The improvement of pollutant degradation was initially increased with the increase of metal content, but it decreased when the metal content reached a high level.[41–43] As matter of fact, in In,V-codoped TiO_2 catalysts with metal content higher than 0.2%, the metal ions act as electron–hole recombination centres, which as a result decreases the photo-efficiency and photocatalytic activity.

To investigate the In^{3+} doping effect on the photocatalytic performance of TiO_2, it was found that loading indium ions onto TiO_2 particles prevents the particle growth and In^{3+} changes to In^{2+} as electron gets trapped by forming a low energy level between the CB and VB of TiO_2. In the absence of light irradiation, In^{2+} ions convert to In^{3+} and atmospheric O_2 traps the released electrons as electron acceptors to produce O_2^-. The mechanism of this process is shown below:

$$TiO_2 + h\nu \rightarrow TiO_2^{\cdot} + e^- \quad (5)$$

$$In^{3+} + e^- \rightarrow In^{2+} \quad (6)$$

Table 2 The photocatalytic results of MO degradation using In-doped TiO_2 nanoparticles with various In(III) content, prepared *via* sol–gel assisted photochemical deposition

UV light illumination				
Time (min)	15	30	45	60
Elem. (%)				
0	43.67	67.66	81.02	91.02
0.1	45.08	68.36	82.66	91.48
0.2	45.08	68.36	82.66	91.48
0.4	38.20	64.76	76.48	81.95
0.6	40.93	67.11	78.52	89.76
1	45.08	69.53	85.55	92.97
2	49.14	71.01	91.09	96.09

Visible light illumination					
Time (min)	30	60	90	120	150
Elem. (%)					
0	20	30	42.50	52.71	61.20
0.1	12.86	25.50	41.53	48.57	53.43
0.2	30.86	52.21	69.28	83.57	92.50
0.4	27.28	47.14	52.93	70.81	80.28
0.6	21.71	45.32	60.15	64.71	74.86
1	19	27.93	41.25	50.28	57.36
2	26.36	42.07	57.07	68.43	81.92

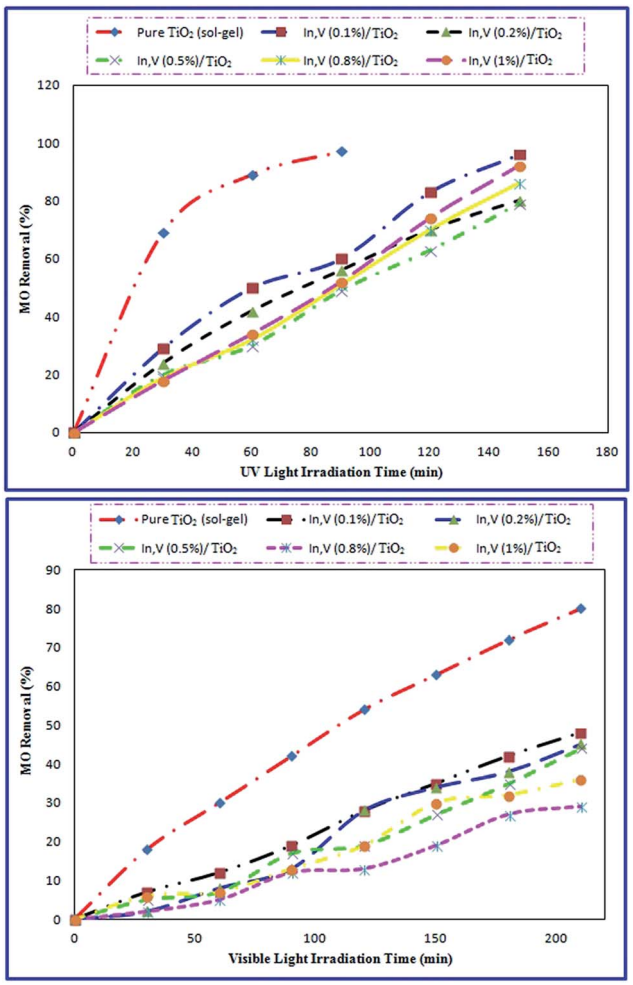

Fig. 7 Photocatalytic activity of pure TiO_2 and In,V-codoped TiO_2 catalysts prepared by sol–gel method, under UV and visible light irradiation.

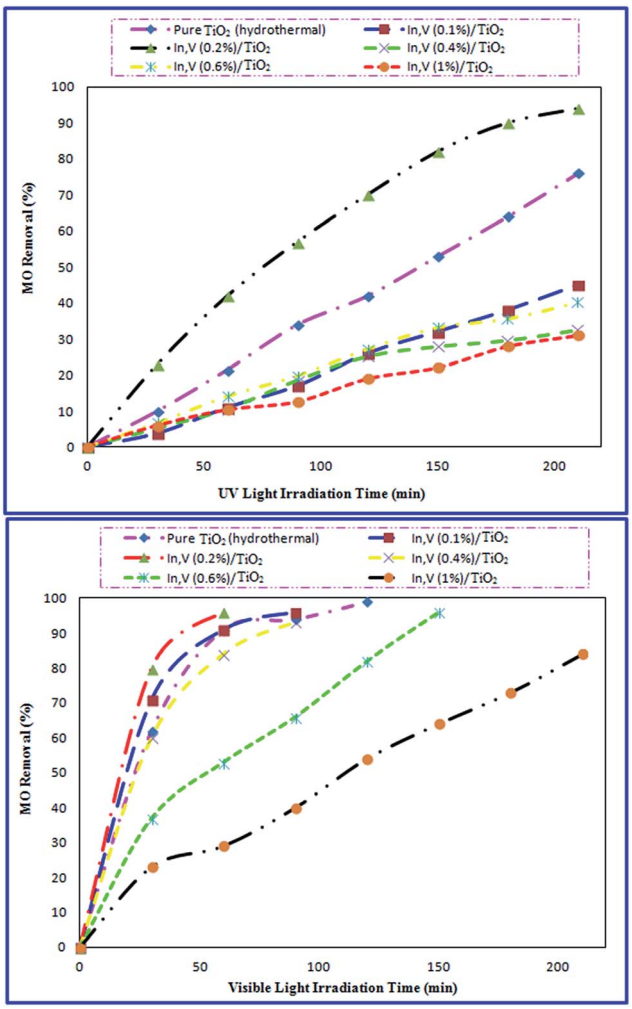

Fig. 8 Photocatalytic activity of pure TiO_2 and In,V-codoped TiO_2 catalysts prepared by hydrothermal method, under UV and visible light irradiation.

$$In^{2+} + \text{oxidation} \rightarrow In^{3+} + e^- \quad (7)$$

$$O_2 + e^- \rightarrow O_2^- \quad (8)$$

In fact, this metal–TiO_2 support interface is largely beneficial for the photocatalytic reactions. The close contact of metal nanoclusters with TiO_2 nanoparticles allows the photogenerated electrons (free or trapped) in TiO_2 lattices (eqn (9) and (10)) to be transferred to the metal lattices (eqn (11) and (12)) easily;

$$TiO_2 + h\nu \rightarrow e_{CB}^- + h_{VB}^+ \quad (9)$$

$$Ti^{4+} + e_{CB}^- \rightarrow Ti^{3+} \quad (10)$$

$$M + e_{CB}^- \rightarrow M^- \quad (11)$$

$$Ti^{3+} + M \rightarrow Ti^{4+} + M^- \quad (12)$$

where $h\nu$ represents the light irradiation energy, e_{CB}^- and h_{VB}^+ represent the photogenerated electrons in CB and holes in the VB of TiO_2, respectively. Ti^{n+} and M_m^- represent the titanium ions or atoms in the TiO_2 crystal and metal atoms or ions in the metallic clusters, respectively.

The number of electrons in the bulk TiO_2 is reduced, thereby the possibility of recombination (eqn (13) and (14)) declines:

$$e_{CB}^- + h_{VB}^+ \rightarrow \text{recombination} \quad (13)$$

$$Ti^{3+} + h_{VB}^+ \rightarrow Ti^{4+} \quad (14)$$

In general, most of the photogenerated electrons and holes recombine through processes in eqn (13) and (14), and only a small number remains for the photocatalytic reactions. By using IR spectroscopy, it was reported that electron transfer from the TiO_2 support to the deposited metal clusters is the bottleneck of the photocatalytic reactions.[44]

Based on our findings, there is a significant potential to enhance efficiency of photocatalytic reactions through improving charge separation and charge transfer using proper metal nanoclusters loading over TiO_2 catalysts.

4. Conclusions

In the current study, a series of novel In,V-codoped TiO_2 catalysts with different In and V contents were synthesized by a photochemical reduction technique and used as photocatalysts to decompose MO as a probe pollutant in an aqueous solution. XRD and EDX analysis did not show any peaks to confirm the appearance of unwanted impurities. SEM analysis confirmed that all samples are uniform, globular and slightly agglomerated and TEM analysis confirmed the results obtained from SEM and XRD analysis. The photocatalytic activity of pure TiO_2 is greatly improved in the presence of loaded metal nanoclusters with 0.2% In and 0.2% V content. The high visible-light-driven photocatalytic activity of In and V modified TiO_2 is ascribed to the synergetic effects of (1) decreased particle size, (2) improved visible-light harvesting ability due to formation of sub-energy levels in the TiO_2 structure, and (3) increased efficiency in separation of photogenerated charge carriers. This investigation contributes to understanding the effects of the complex ion doping on TiO_2 photoactivity and thus provides a reference for improving its environmental application.

Acknowledgements

We are grateful to the Council of University of Kashan, the Iran Nanotechnology Initiative Council and the University of Texas at El Paso (UTEP) for providing financial support. We also thank Dr Peter Cooke from New Mexico State University (NMSU) and Dr Sudheer Molugu for helping us with TEM measurements, Dr Jing Wu from Texas A & M University for helping us with XPS analysis, Dr Juan Noveron from chemistry department of UTEP for providing us with the UV light reactor, and the College of Engineering at UTEP for allowing access to their SEM, EDX and XRD instruments.

References

1 K. Chen, J. Li, J. Li, Y. Zhang and W. Wang, *Colloids Surf., A*, 2010, **360**, 47.
2 X. Xiao, K. Ouyang, R. Liu and J. Liang, *Appl. Surf. Sci.*, 2009, **255**, 3659.
3 L. Armelao and D. Barreca, *Nanotechnology*, 2007, **18**, 375709.
4 S. Watson, D. Beydoun, J. Scott and R. Amal, *J. Nanopart. Res.*, 2004, **6**, 193.
5 S. Xu, Y. Zhu, L. Jiang and Y. Dan, *Water, Air, Soil Pollut.*, 2010, **213**, 151.
6 E. Khelifi, H. Gannoun, Y. Touhami, H. Bouallagui and M. Hamdi, *J. Hazard. Mater.*, 2008, **152**, 683.
7 S. Kim, S. Hwang and W. Choi, *J. Phys. Chem. B*, 2005, **109**, 24260.
8 O. Rosseler, M. Shankar, K.-L. Dum, L. Schmidlin, N. Keller and V. Keller, *J. Catal.*, 2010, **269**, 179.
9 M. Hamadanian, S. Karimzadeh, V. Jabbari and D. Villagrán, *Mater. Sci. Semicond. Process.*, 2015, in press.
10 N. Murakami, T. Chiyoya, T. Tsubota and T. Ohno, *Appl. Catal., A*, 2008, **348**, 148.
11 L. G. Devi, B. N. Murthy and S. G. Kumar, *Mater. Sci. Eng., B*, 2010, **166**, 1.
12 M. Hamadanian, A. S. Sarabi, A. Mihammadi Mehra and V. Jabbari, *Appl. Surf. Sci.*, 2011, **257**, 10639.
13 M. Hamadanian, V. Jabbari and M. Shamshiri, *Appl. Surf. Sci.*, 2014, **317**, 302.
14 D. M. Chen, D. Yang, Q. Wang and Z. Y. Jiang, *Ind. Eng. Chem. Res.*, 2006, **45**, 4110.
15 O. Carp, C. L. Huisman and A. Reller, *Prog. Solid State Chem.*, 2004, **32**, 33.
16 H. S. Hilal, L. Z. Majjad, N. Zaatar and A. El-Hamouz, *Solid State Sci.*, 2007, **9**, 9.
17 D. Jiang, Y. Xu, B. Hou, D. Wu and Y. J. Sun, *Solid State Chem.*, 2007, **180**, 1787.
18 B. Liu, X. Zhao, N. Zhang, Q. Zhao, X. He and J. Feng, *Surf. Sci.*, 2005, **595**, 203.
19 A. Dawson and P. V. Kamat, *J. Phys. Chem.*, 2001, **105**, 960.
20 A. Molinari, R. Amadelli, L. Antolini, A. Maldatti, P. Battioni and D. Mansuy, *J. Mol. Catal. A: Chem.*, 2000, **158**, 521.
21 D. Bahnemann, A. Henglein, J. Lilie and L. Spanhel, *J. Phys. Chem.*, 1984, **88**, 709.
22 O. V. Makarova, T. Rajh, M. C. Thurnauer, A. Martin, P. A. Kemme and D. Cropek, *Environ. Sci. Technol.*, 2000, **34**, 4797.
23 D. Raftery and S. Klosek, *J. Phys. Chem. B*, 2001, **105**, 2815.
24 J. C.-S. Wu and C. H. Chen, *J. Photochem. Photobiol., A*, 2004, **163**, 509.
25 W. Y. Choi, A. Termin and M. R. J. Hoffmann, *J. Phys. Chem.*, 1994, **98**, 13669.
26 E. Wang, W. Yang and Y. Cao, *J. Phys. Chem. C*, 2009, **113**, 20912.
27 B. S. Liu, X. Zhao, N. Zhang, Q. Zhao, X. He and J. Feng, *Surf. Sci.*, 2005, **595**, 203.
28 R. Estrellan, C. Salim and H. Hinode, *J. Hazard. Mater.*, 2010, **179**, 79.
29 N. Serpone, *J. Phys. Chem. B*, 2006, **110**, 24287.
30 R. Zhang, Y. H. Kim and Y. S. Kang, *Curr. Appl. Phys.*, 2006, **6**, 801.
31 S. Dong, C. Tang, H. Zhou and H. Zhao, *Gold Bull.*, 2004, **37**, 3.
32 M. Hamadanian, A. Reisi-Vanani and A. Majedi, *Mater. Chem. Phys.*, 2009, **116**, 376.
33 J. H. Kim, B. H. Noh, G. D. Lee and S. S. Hong, *Korean J. Chem. Eng.*, 2005, **22**, 370.
34 D. Li, H. Haneda, S. Hishita and N. Ohashi, *Chem. Mater.*, 2005, **17**, 2588.
35 J. Zhang, J. Xiab and Z. Ji, *J. Mater. Chem.*, 2012, **22**, 17700.
36 M. Hamadanian, M. Amani and V. Jabbari, *Polym.-Plast. Technol. Eng.*, 2014, **53**, 1283.
37 Wu-Q. Wu, H.-S. Rao, Y.-F. Xu, Yu-F. Wang, C.-Y. Su and D.-B. Kuang, *Sci. Rep.*, 2013, **3**, 1892.
38 J. Li, J. Xu and J. Huang, *CrystEngComm*, 2014, **16**, 375.
39 J. Gan, *et al.*, *Sci. Rep.*, 2013, **3**, 1021.
40 E. P. Reddy, L. Davydov and P. G. Smirniots, *J. Phys. Chem. B*, 2002, **106**, 3394.
41 X. Yang, L. Xu, X. Yu and Y. Guo, *Catal. Commun.*, 2008, **9**, 1224.
42 J. Xie, X. Lu, M. Chen, G. Zhao, Y. Song and S. Lu, *Dyes Pigm.*, 2008, **77**, 43.
43 A. Mills and M. McGrady, *J. Photochem. Photobiol., A*, 2008, **193**, 228.
44 J. Zhu, W. Zheng, B. He, J. Zhang and M. Anpo, *J. Mol. Catal. A: Chem.*, 2004, **216**, 35.